Supporting Information

Electrochemically Deposited Sn Catalysts with Dense Tips on Gas Diffusion Electrode for Electrochemical CO_2 Reduction

Jinkyu Lim, Phil Woong Kang, Sun Seo Jeon, and Hyunjoo Lee*

Department of Chemical and Biomolecular Engineering, Korea Advanced Institute of Science and Technology, Daejeon 34141, South Korea

Corresponding Author

E-mail: azhyun@kaist.ac.kr (H. Lee)

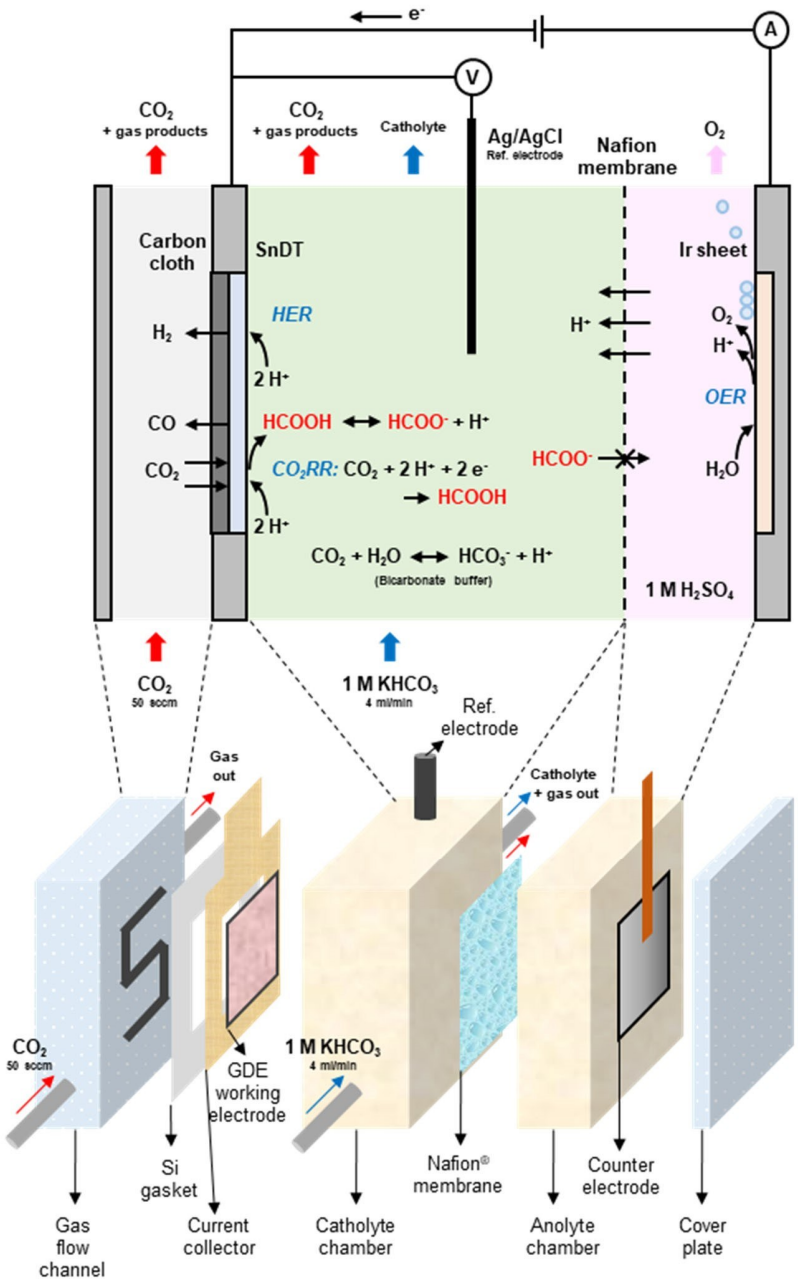

Fig. S1 A schematic diagram of the customized GDE electrolysis cell. The gas flow chamber had a flow channel. The working electrode, membrane, and counter electrode were placed in parallel. The outgoing gas from the gas chamber and the catholyte chamber was combined and its composition was measured by GC. Liquid products were collected in only catholyte. Silicon sheet or Viton O-rings were placed between each part when they were assembled.

Table S1 The measured pH values of the catholytes.

$KHCO_3$ concentration	As-prepared	CO_2-saturated	Under the CO_2RR condition
0.1 M	8.7	6.8	6.4
0.5 M	8.5	7.4	7.4
1.0 M	8.4	7.8	7.8
2.0 M	8.3	8.2	8.2

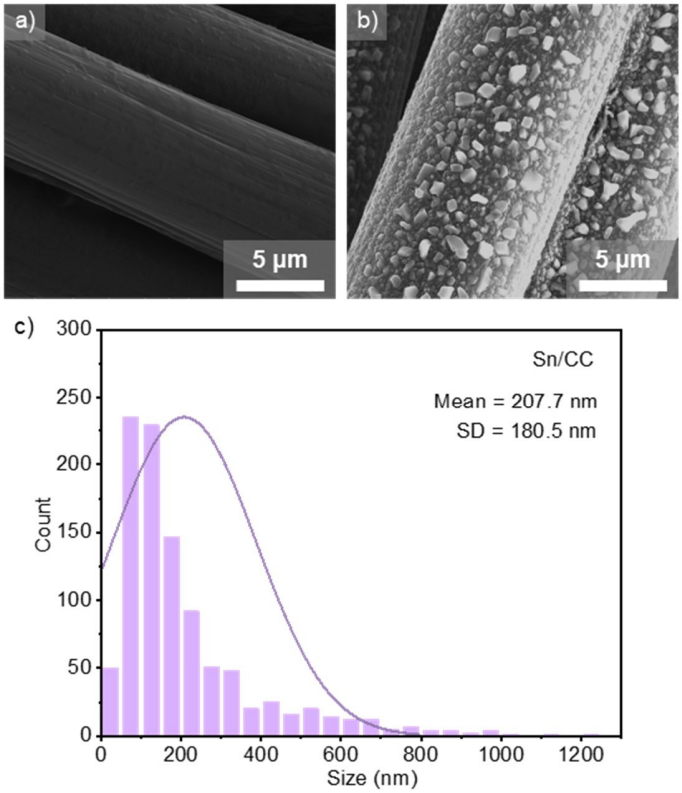

Fig. S2 SEM images of a) bare carbon cloth (CC) substrate and b) Sn layer-coated CC (Sn/CC) electrode prepared by E-beam deposition. c) Particle size distribution of Sn domain in Sn/CC electrode. Over a thousand of the Sn particles were investigated. Average size was 207.7 nm, and the standard deviation was 180.5 nm.

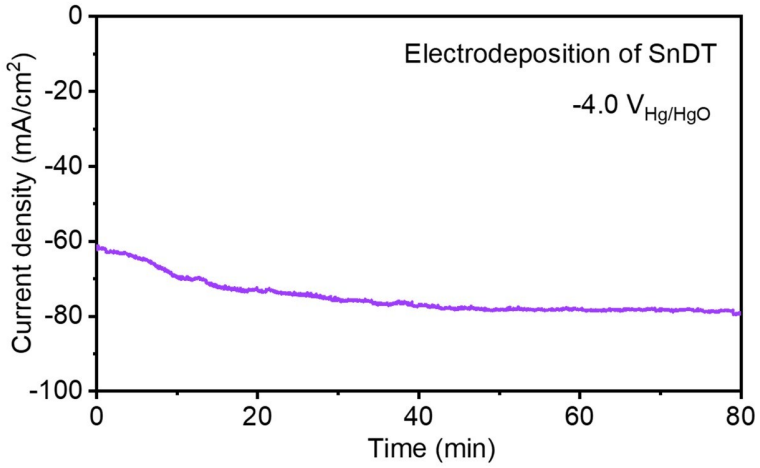

Fig. S3 Transient current density during the electrodeposition of SnDT on the Sn/CC substrate. The plating solution was 0.5 M $Na_2SnO_3 \cdot 3H_2O$ and 0.4 M NaOH. Basic plating solution was needed to preserve Sn thin layer and have high uniformity over large area. A Hg/HgO reference electrode and a Sn wire counter electrode were used. The temperature of the solution was controlled to 25 °C.

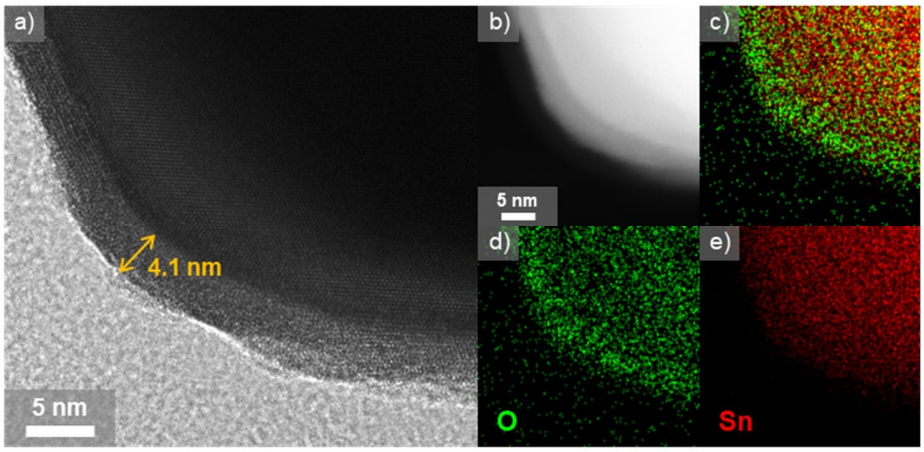

Fig. S4 TEM analysis for a tip of the SnDT catalyst with atomic resolution. (a) A HR-TEM image, and (b) a HAADF-STEM image. The surface native oxide layer had 4.1 nm thickness. The EDS mapping images; (c) overlapped image, (d) O distribution, and (e) Sn distribution.

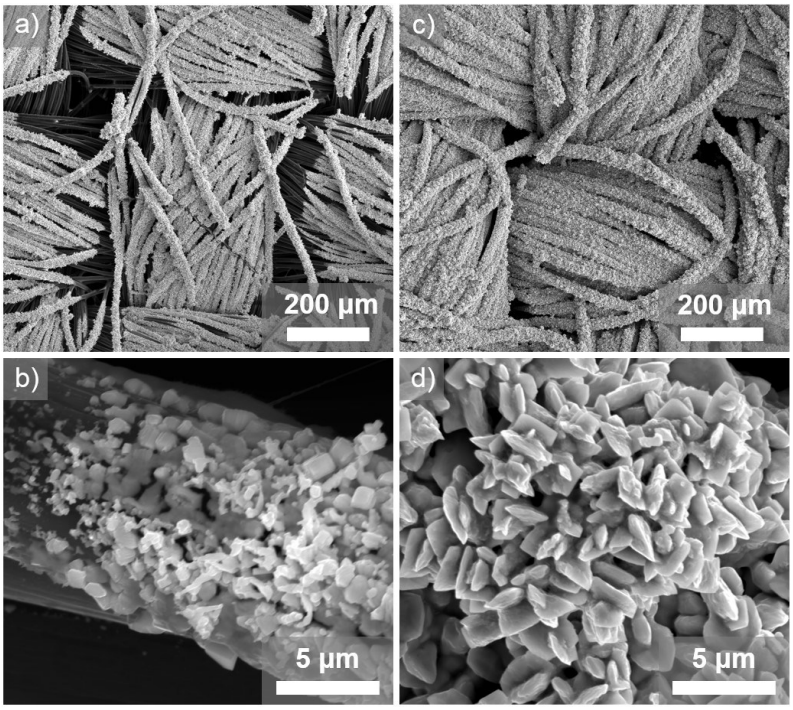

Fig. S5 SEM images of electrodeposited SnDT catalysts on a) and b) a bare CC substrate, c) and d) a Sn/CC substrate.

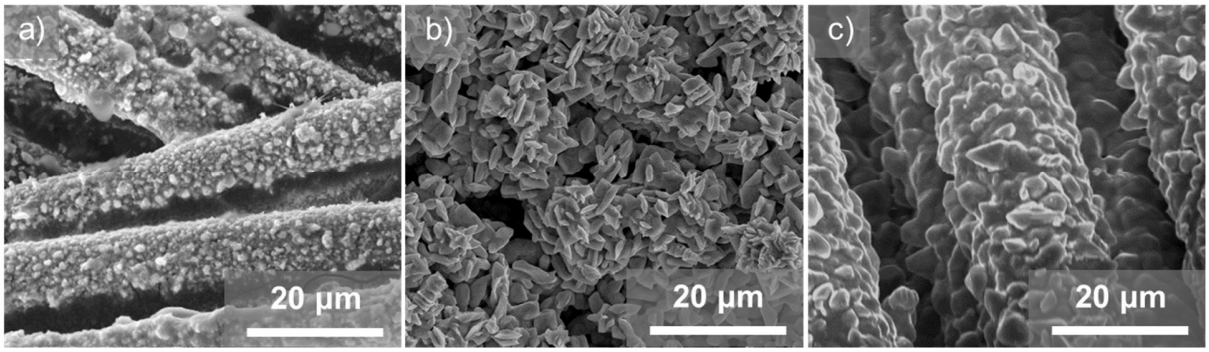

Fig. S6 SEM images of the SnDT electrodes prepared at various electrodeposition temperatures. a) At 0 °C, there was less deposition of Sn due to huge HER. b) At 25 °C, optimum SnDT catalysts with the nanostructured surface were obtained. c) At 55 °C, the surface had a comparatively flat surface.

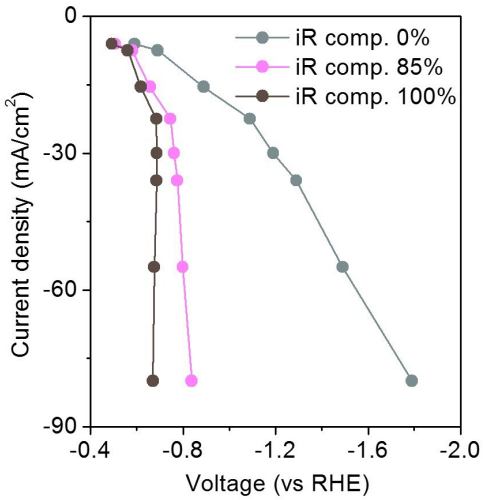

Fig. S7 Polarization curves of the SnDT with various degrees of iR compensation. To avoid overcompensation, 85 % iR compensation was used in this work. The catholyte was CO_2-saturated 1 M $KHCO_{3(aq)}$ with magnetic stirring, and the anolyte was 1 M $H_2SO_{4(aq)}$. Ir sheet anode and Nafion® 212 membrane were used. The ambient temperature and pressure were maintained. Each point was obtained from 30 min of potentiostatic operations.

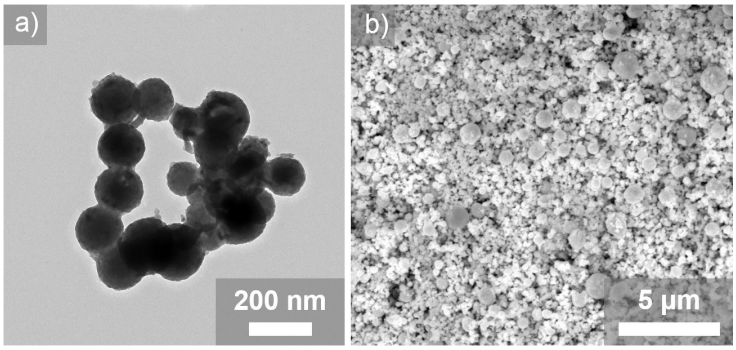

Fig. S8 a) TEM and b) SEM images of commercial Sn nanopowders (SnNP, Sigma Aldrich)

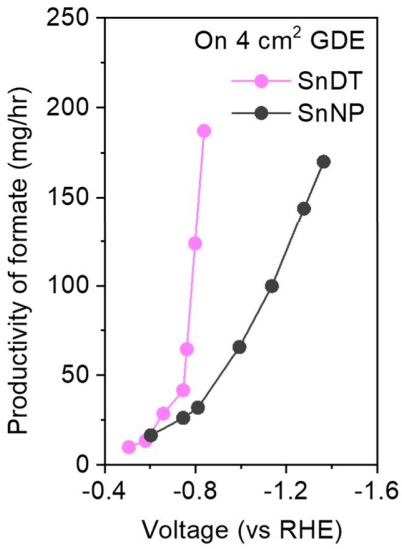

Fig. S9 Formate productivity with the customized GDE cell and SnDT or SnNP electrocatalysts. The geometric area of the cathode was 4 cm^2. The catholyte was stagnant CO_2-saturated 1 M $KHCO_{3(aq)}$ with magnetic stirring, and the anolyte was 1 M $H_2SO_{4(aq)}$. Ir sheet anode and Nafion® 212 membrane were used. The ambient temperature and pressure were maintained. Each point was obtained from 30 min of potentiostatic operations.

Table S2 The comparison of formate productivity from CO_2RR using various catalysts in literatures.

Catalysts	Formate productivity (mg/hr)	Voltage (vs RHE)	iR comp.	Electrode type	Electrode size (cm^2)	Aqueous catholyte	Reference
Electrodeposited Sn with dense tips (SnDT)	**65**	**-0.76 V**	**O (85 %)**	**GDE**	**4**	**1.0 M $KHCO_3$**	**This work**
Electrodeposited Sn with dense tips (SnDT)	**188**	**-0.84 V**	**O (85 %)**	**GDE**	**4**	**1.0 M $KHCO_3$**	**This work**
Ni doped SnS_2 nanosheets	6.4	-0.9 V	O	Planar electrode	0.5	0.1 M $KHCO_3$	Angew. Chem. Int. Ed. 2018, 57, 1095410958.
Cu-SnO_2 core-shell / C	4	-0.7 V	N. A.	Planar electrode	0.49	0.5 M $KHCO_3$	J. Am. Chem. Soc. 2017, 139, 42904293.
AgSn/SnO_x coreshell	11	-1.06 V	O	Planar electrode	0.5	0.5 M $NaHCO_3$	J. Am. Chem. Soc. 2017, 139, 18851893.
Pd-B/C	1	-0.5 V	N. A.	Planar electrode	0.2	0.1 M $KHCO_3$	J. Am. Chem. Soc. 2018, 140, 28802889.
Bi-Sn bimetallic alloy	45	-1.14 V	N. A.	Planar electrode	1	0.5 M $KHCO_3$	Adv. Energy Mater. 2018, 8, 1802427.
Hierarchical Sn dendrites	3	-1.36 V	N. A.	Planar electrode	0.13	0.1 M $KHCO_3$	ChemSusChem 2015, 8, 3092-3098.
SnO_2 quantum wires	9.4	-0.82 V	O	Planar electrode	0.785	0.1 M $KHCO_3$	Angew. Chem. Int. Ed. 2019, 58, 84998503.
Hierarchical mesoporous SnO_2 nanosheets	108	-1.0 V	N. A.	Planar electrode	3	0.5 M $NaHCO_3$	Angew. Chem. Int. Ed. 2017, 56, 505-509.
Reduced SnO_2 porous nanowires	31	-1.0 V	O (85 %)	Planar electrode	5	0.1 M $KHCO_3$	Angew. Chem. Int. Ed. 2017, 56, 36453649.
Ultra small SnO nanoparticles	17	-0.87 V	N. A.	Planar electrode	1	0.5 M $KHCO_3$	Angew. Chem. Int. Ed. 2018, 57, 29432947.

Sn nanoparticles	59	-1.2 V	N. A.	GDE	7	0.5 M $KHCO_3$	RSC Adv. 2014, 4, 5997059976.
Sn nanoparticles	100	-1.2 V	N. A.	GDE	7	0.1 M $KHCO_3$	J. Power Sources 2014, 271, 278-284.
Sn powders	140	-1.15 V	N. A.	GDE	9	0.5 M $NaHCO_3$	J. Power Sources 2013, 223, 68-73.
Sn nanoparticles	130	-1.4 V	N. A.	GDE	7	0.5 M $KHCO_3$	J. Power Sources 2015, 279, 1-5.
Hierarchical SnO_2 microsphere	25	-0.9 V	N. A.	GDE	4	0.5 M $KHCO_3$	Appl. Energy 2016, 175, 536-544.
Sn nanoparticles / C	95	-1.1 V	N. A.	GDE	1	0.45 M $KHCO_3$ + 0.5 M KCl	J. CO_2. Util. 2017, 18, 222-228.
SnO_2 nanoparticles	0.4	-0.8 V	O	GDE	0.01	1.0 M KOH	J. Mater. Chem. A 2018, 6, 1031310319.
SnO_2 nanoparticles	0.6	-1.03 V	O	GDE	0.01	1.0 M KOH	J. Mater. Chem. A 2018, 6, 1031310319.

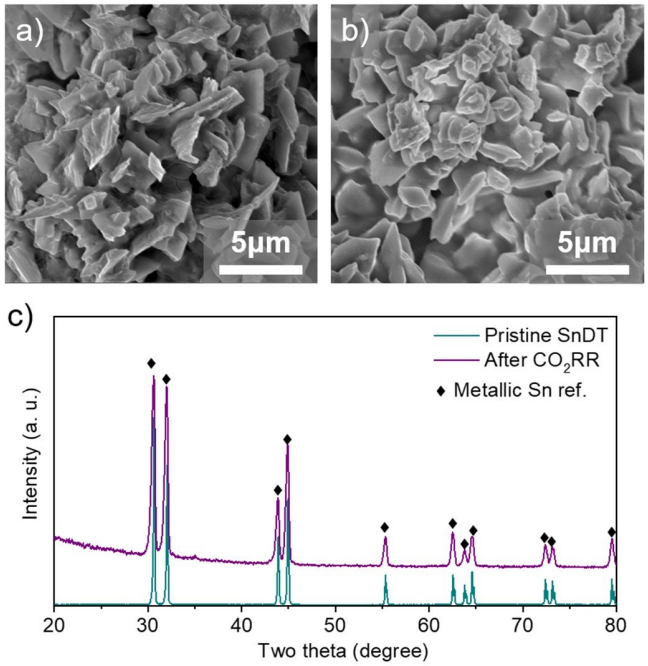

Fig. S10 SEM images of the SnDT electrodes a) before and b) after the durability test performed at -0.76 V_{RHE} for 72 h. c) XRD spectra obtained before and after the durability test. The catholyte was CO_2-saturated 1 M $KHCO_{3(aq)}$ under circulation, and the anolyte was 1 M $H_2SO_{4(aq)}$. Ir sheet anode and Nafion® 212 membrane were used. The ambient temperature and pressure were maintained.

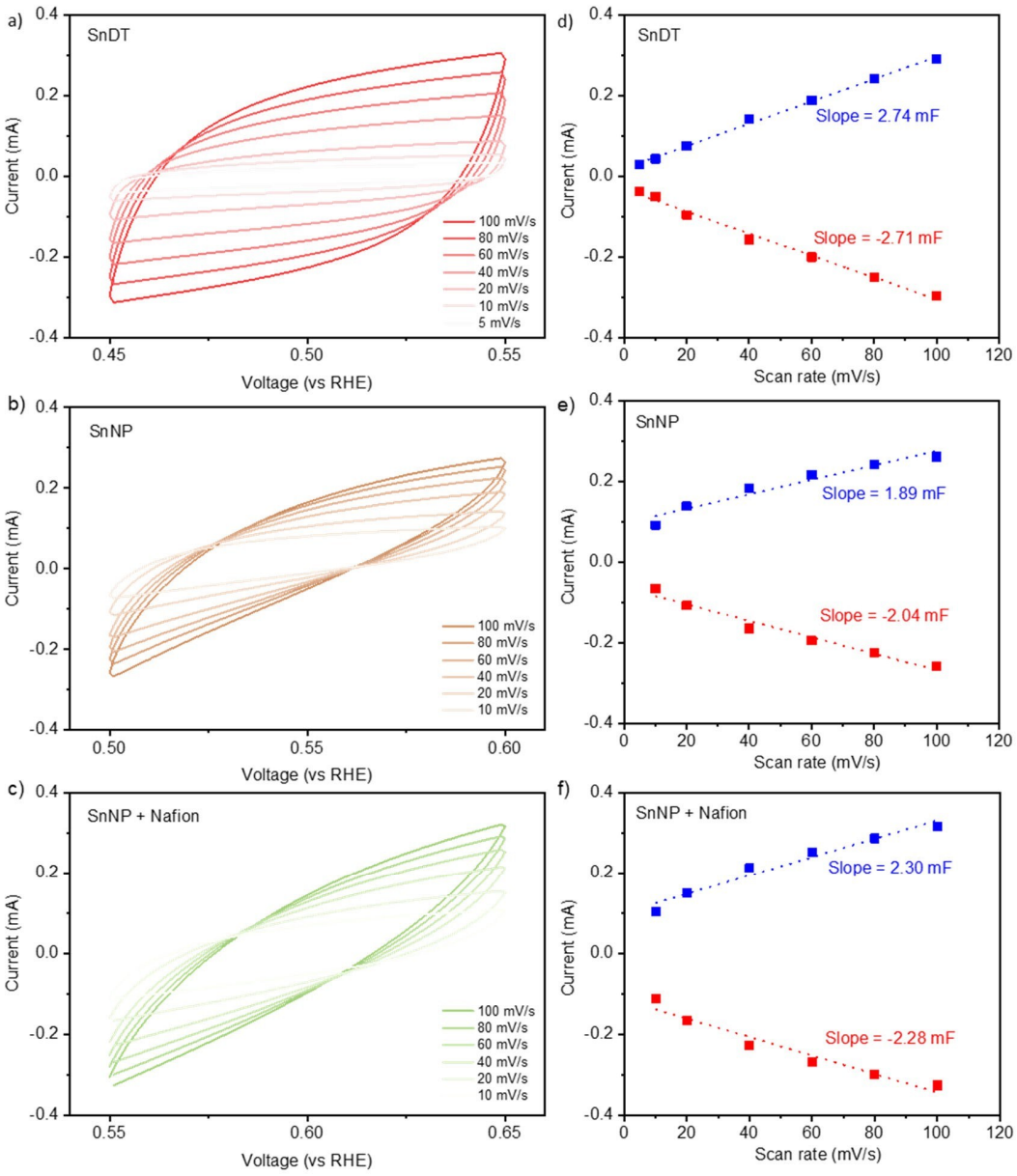

Fig. S11 Electrochemical surface area (ECSA) estimation after the CO_2RR operations. a), b), c) Cyclic voltammetry cycles with different scan rates, and d), e), f) current-scan rate plots to estimate double layer capacitances for SnDT, SnNP, and SnNP with 10 % ionomer electrodes, respectively. CO_2-saturated 1M $KHCO_{3(aq)}$ electrolyte, a graphite sheet counter electrode, and an Ag/AgCl (3M NaCl) reference electrode were used. The geometric area of the electrodes was 4 cm^2.

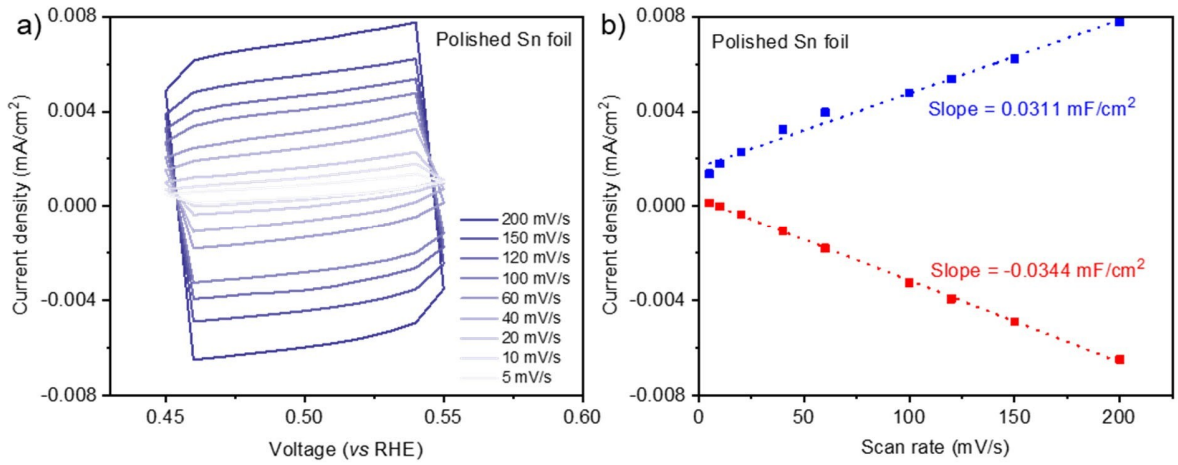

Fig. S12 Specific capacitance (C_S) estimation for CO_2-saturated 1.0 M $KHCO_{3(aq)}$ with a polished Sn foil (Alfa Aesar, 99.9985%). a) Cyclic voltammetry cycles at different scan rates, and b) current density-scan rate plots to estimate double layer capacitance. It was assumed that the polished Sn foil had atomically smooth planes. CO_2-saturated 1M $KHCO_{3(aq)}$ electrolyte, a graphite sheet counter electrode, and an Ag/AgCl (3M NaCl) reference electrode were used. The geometric area of the electrode was 4 cm^2.

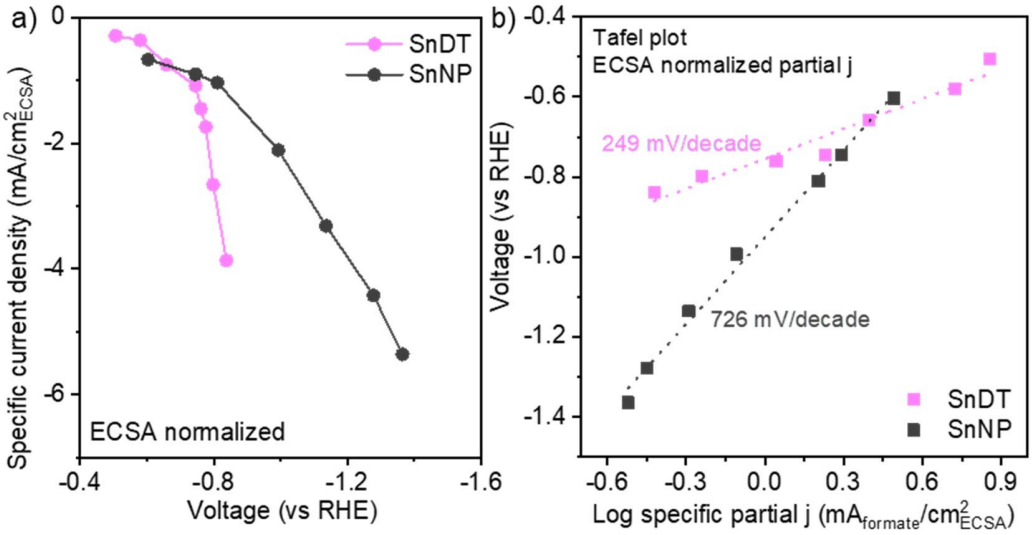

Fig. S13 (a) j-V curves normalized by ECSA for SnDT and SnNP catalysts. The ECSA values for each electrode were 82.7 cm^2, and 59.7 cm^2 for SnDT and SnNP, respectively. (b) Tafel plots for the ECSAnormalized partial current density toward formate for SnDT and SnNP catalysts. The catholyte was stagnant CO_2-saturated 1 M $KHCO_{3(aq)}$ with magnetic stirring, and the anolyte was 1 M $H_2SO_{4(aq)}$. Ir sheet anode and Nafion® 212 membrane were used. The ambient temperature and pressure were maintained. Each point was obtained from 30 min of potentiostatic operations. The geometric areas of the electrodes were 4 cm^2.

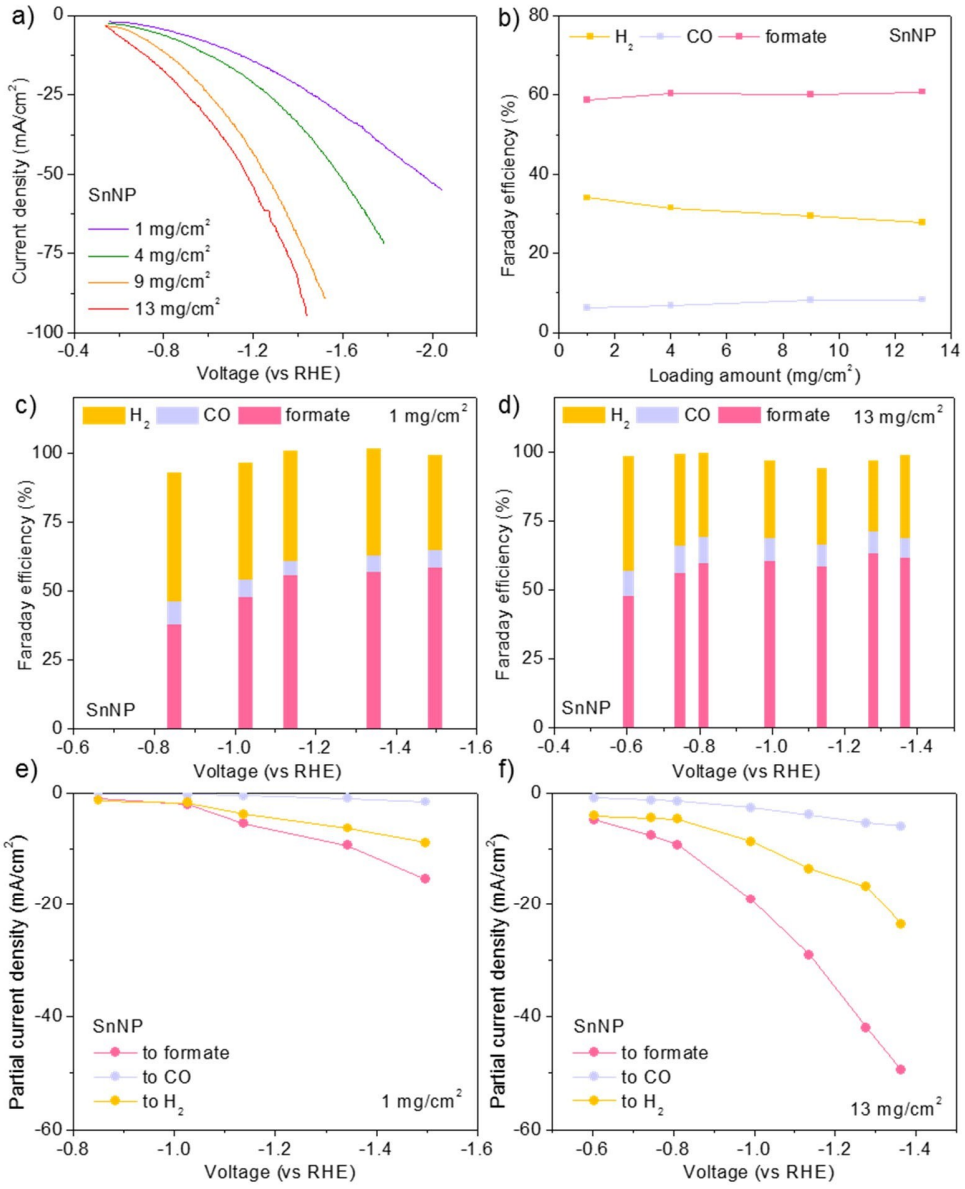

Fig. S14 Electrochemical analyses of SnNP electrodes with different Sn loadings. SnNP was gently sprayed using a N_2 spray without polymeric additives. a) Linear sweep voltammetry scans with different loadings of SnNP at scan rate of 50 mV/s. SnNP could not be deposited more than 13 mg/cm^2. b) Product distributions of SnNP electrodes with different loadings at -30 mA/cm^2. c), d) Product distributions, and e), f) partial current density toward each product at different overpotentials for 1 mg/cm^2 and 13 mg/cm^2 SnNP loadings, respectively. Each point was obtained from 30 min of potentiostatic operations. The catholyte was stagnant CO_2-saturated 1 M $KHCO_{3(aq)}$ with magnetic stirring, and the anolyte was 1 M $H_2SO_{4(aq)}$. Ir sheet anode and Nafion® 212 membrane were used. The ambient temperature and pressure were maintained.

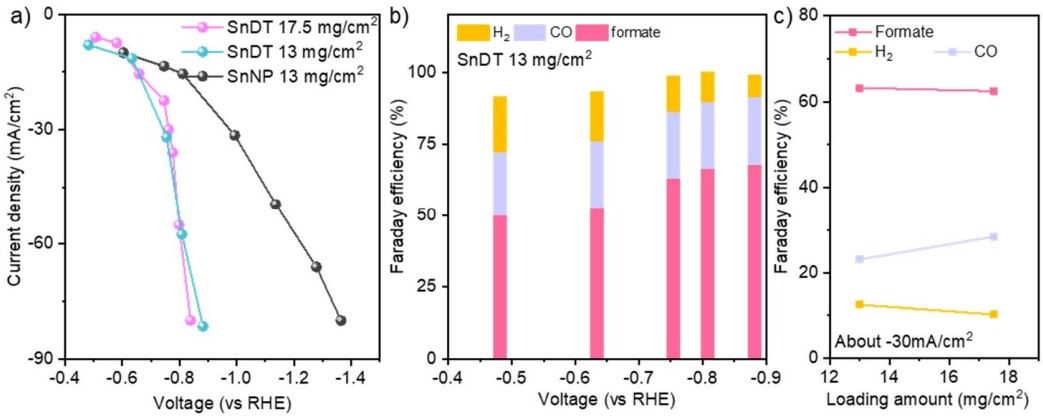

Fig. S15 CO_2RR results on the SnDT electrode with the reduced loading amount of 13 mg_{Sn}/cm^2. (a) j-V curves with the results from the SnDT (17.5 mg/cm^2) and the SnNP (13 mg/cm^2). (b) Product distribution for the SnDT with 13 mg/cm^2 at various applied potentials. (c) Product distributions at -30 mA/cm^2 with different loadings. The catholyte was CO_2-saturated 1 M $KHCO_3$(aq) and the anolyte was 1 M H_2SO_4(aq). Ir sheet anode and Nafion® 212 membrane were used. The ambient temperature and pressure were maintained.

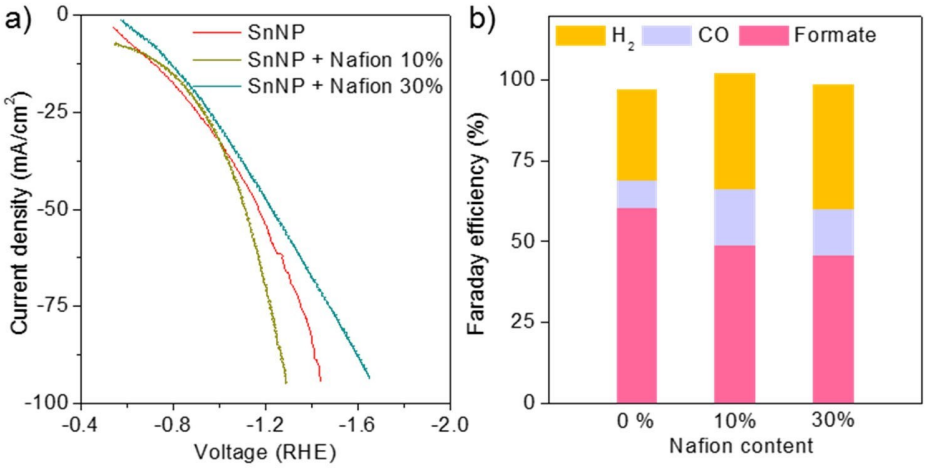

Fig. S16 CO_2RR with SnNP with different contents of Nafion ionomer from 0 % to 30 %. a) Linear sweep voltammetry with a scan rate of 50 mV/s. b) Product distributions at -30 mA/cm^2. The SnNP loading was 13 mg/cm^2. The catholyte was stagnant CO_2-saturated 1 M $KHCO_{3(aq)}$ with magnetic stirring, and the anolyte was 1 M $H_2SO_{4(aq)}$. Ir sheet anode and Nafion® 212 membrane were used. The ambient temperature and pressure were maintained.

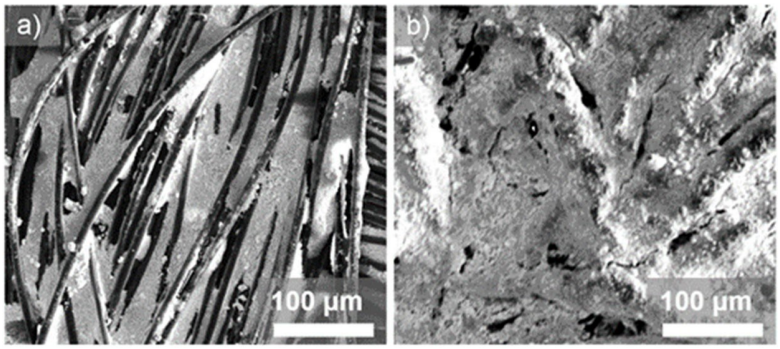

Fig. S17 SEM images of a) SnNP electrode without polymer additives and b) SnNP electrode sprayed with 10 wt% Nafion ionomer. The loading of SnNP were 13 mg/cm^2 in both electrodes.

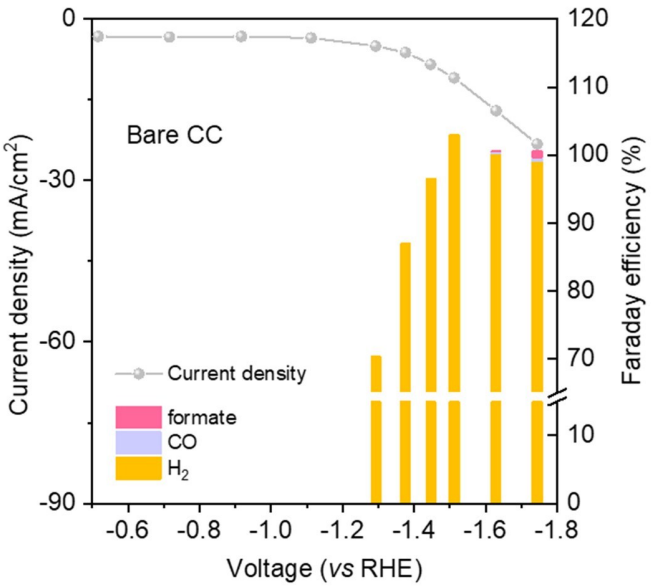

Fig. S18 Current density and Faradaic efficiency of bare CC substrate under CO_2 flow. The catholyte was stagnant CO_2-saturated 1 M $KHCO_{3(aq)}$ and the anolyte was 1 M $H_2SO_{4(aq)}$. Ir sheet anode and Nafion® 212 membrane were used. The geometric area of the GDE was 4 cm^2. Each point on the j-V curve was obtained from 30 min of potentiostatic operations.

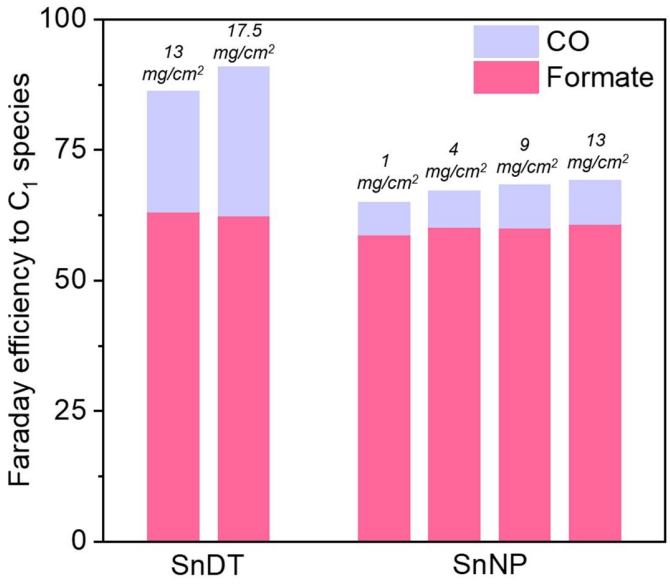

Fig. S19 Faradaic efficiency to C_1 species on the SnDT or the SnNP electrodes with various Sn metal loading amounts at the current density of -30 mA/cm^2. The catholyte was stagnant CO_2-saturated 1 M $KHCO_{3(aq)}$ with magnetic stirring, and the anolyte was 1 M $H_2SO_{4(aq)}$. Ir sheet anode and Nafion® 212 membrane were used. The ambient temperature and pressure were maintained.

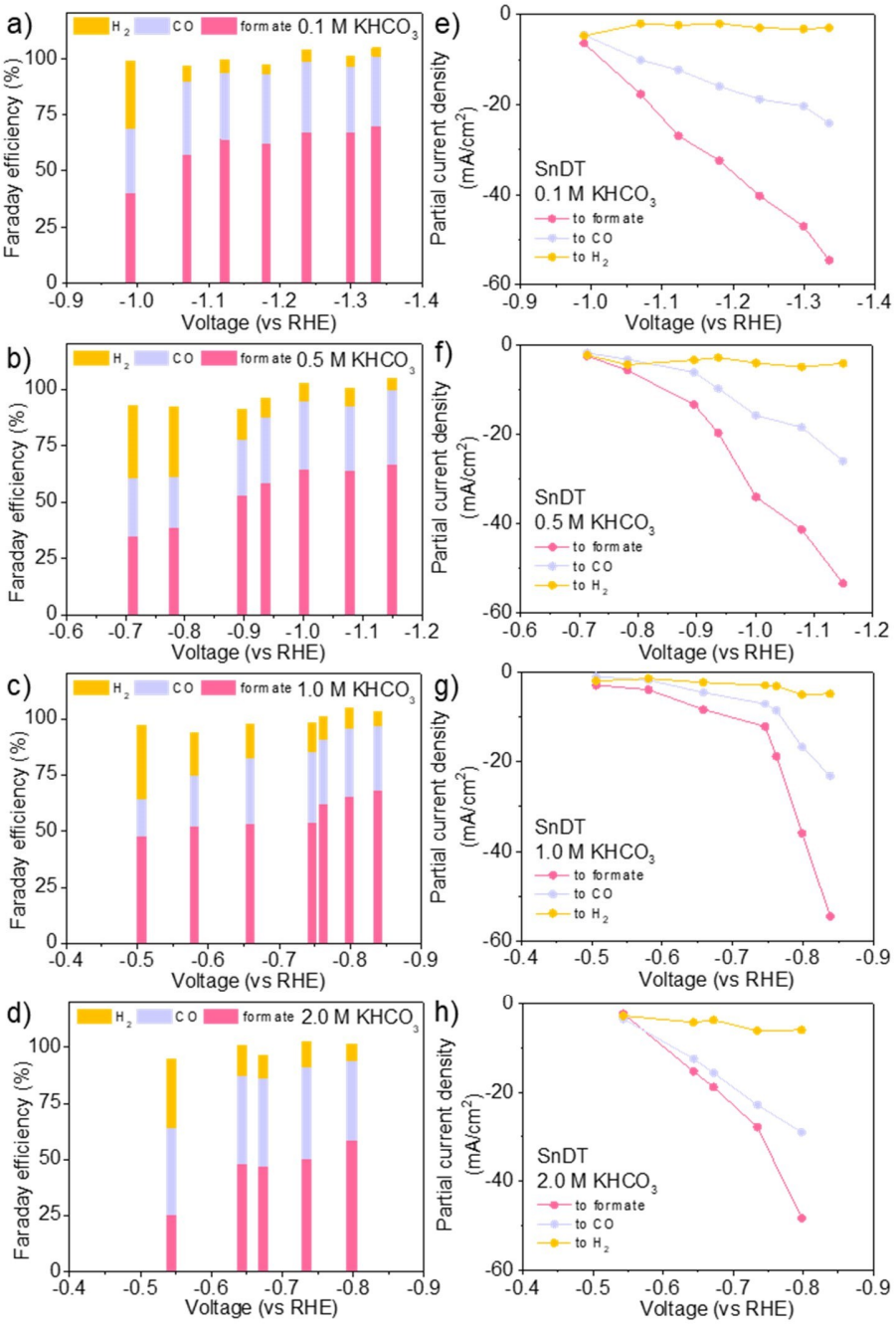

Fig. S20 a), b), c), d) Product distributions and e), f), g), h) partial current densities on the SnDT electrode in CO_2-saturated 0.1 M, 0.5 M, 1.0 M, and 2.0 M of $KHCO_{3(aq)}$ with magnetic stirring, respectively. The anolyte was 1 M $H_2SO_{4(aq)}$. Ir sheet anode and Nafion® 212 membrane were used. The ambient temperature and pressure were maintained. Each point was obtained from 30 min of potentiostatic operations.